Radiation Measurements 138 (2020) 106229

Contents lists available at ScienceDirect

Radiation Measurements

journal homepage: http://www.elsevier.com/locate/radmeas

Review

Timepix-based detectors in mixed-field charged-particle radiation dosimetry applications

Lawrence S. Pinsky *, Stanislav Pospisil

ABSTRACT

Timepix-based detectors have been deployed in a variety of mixed-field situations for dosimetry applications, such as Radon monitoring, evaluating propagating hadron therapy beams, and assessing radiation doses received by airline passengers and crewmembers. However, one of the most significant and complex achievements of Timepix-based detectors is their success in evaluating the incident charged particle fields in space radiation environments, both inside spacecraft and exposed to space with minimal shielding. This paper documents the applications of Timepix-based instruments for the purpose of determining the radiation doses experienced by astronauts. The incident neutron and to a much lesser extent, the dosimetric relevant photon component of that radiation field are not addressed in this review article. Timepix-based detectors have been deployed in a variety of mixed-field situations for dosimetry applications, such as Radon monitoring, evaluating propagating hadron therapy beams, and assessing radiation doses received by airline passengers and crewmembers. However, one of the most significant and complex achievements of Timepix-based detectors is their success in evaluating the incident charged particle fields in space radiation environments, both inside spacecraft and exposed to space with minimal shielding. This paper documents the applications of Timepix-based instruments for the purpose of determining the radiation doses experienced by astronauts. The incident neutron and to a much lesser extent, the dosimetric relevant photon component of that radiation field is addressed separately in this volume.

1. Introduction

The focus of this review on the application of Timepix-based detectors to mixed-field charged-particle dosimetry will concentrate, as a representative example, on the specific applications of Timepix-based devices for dosimetry in the space radiation environment, and in particular specifically assessing the contribution from the ambient charged particle environment. Applications to assess the related ambient incident neutron and high-energy photon dosimetric contributions not addressed in this review article. (Reference to Neutron and) Note that the capabilities of such Timepix-based devices have also found similar applications in a number of other mixed field ground-based (Ploc et al., 2014; Kroupa et al., 2017a; Granja et al., 2018) and atmospheric dosimetric applications such as evaluating hadron therapy beams (Kubančák et al., 2015), Radon monitoring (Caresana et al., 2014) and in assessing radiation doses received by airline passengers and crewmembers (Kubancak et al., 2015).

In 2006, even before the first Timepix wafer had been produced, NASA's Space Radiation Analysis Group at the Johnson Space Center in Houston, Texas surveyed both the then available and the imminently anticipated radiation detector technologies that could be considered for future use in providing dosimetric information in space radiation environments (Semones, 2006). Even at that early stage, the potential capabilities and benefits for employing radiation-imaging detectors in such mixed field dosimetry applications were immediately recognized. The subsequent successes of Timepix-based devices in space have come to validate their judgment (Stoffle et al., 2015; Pinsky et al., 2014; Stoffle, 2013; Kroupa et al., 2015; Granja et al., 2016; Whyntie and Harrison, 2015), but harnessing and optimizing the capabilities of this complex technology for use in such diverse radiation environments has taken a significant effort that will be reviewed in this paper.

Briefly, the radiation environment in space is dominated by several different sources. The Galactic Cosmic Rays (GCR) are basically composed of the energetic bare nuclei of all of the elements on the periodic table. Protons and Helium nuclei comprise ~99% of the GCR, with all of the heavier nuclei (heavy ions) making up only about 1%. The abundances of the heavy ions have a relative peak at Fe and Ni, with all contributions of heavier nuclei combined being several orders of magnitude less than Fe in total. While the heavy ions represent a small portion of the GCR, the fact that their energy loss rate in material such as human tissue is proportional to their charge squared, gives them a very significant cause for dosimetric concern. The energy spectrum of the GCR particles varies with the solar cycle due to interactions with the Heliosphere's magnetic fields, and the solar wind, having a maximum effect at the time of the minimum of the solar sunspot cycle. The energy spectrum nominally peaks at kinetic energies in the 800–1100 MeV range and decreases at higher energies with a power law function of $\sim E^{-2.6}$ (En.wikipedia.org). Other sources of incident radiation include

* Corresponding author.
E-mail address: pinsky@uh.edu (L.S. Pinsky).

https://doi.org/10.1016/j.radmeas.2019.106229
Received 6 February 2019; Accepted 7 December 2019
Available online 11 December 2019
1350-4487/

the Earth's Trapped Radiation Belts, which are composed of protons and electrons, both with energy spectra that are much lower but substantially more intense than that of a typical GCR particle (Van Allen Radiation Belt, 2018). The trapped electron flux is typically not energetic enough to penetrate spacecraft walls, but through bremsstrahlung and excitation interactions with the spacecraft structures, can create x-ray photons that permeate the internal spacecraft volumes. Finally, Solar Particle Events from the Sun can give rise to transient significant fluxes of mostly protons, with some potential for heavier ions, in sufficient numbers and high enough energy to require mitigation provisions to protect astronauts, especially in interplanetary space beyond the geomagnetic field.

Before discussing the detailed issues that need to be addressed to optimize the use of the Timepix in such dosimetric applications several comments are in order regarding space radiation dosimetry itself. First, where the measurement at issue is intended to assess the net risk of harm to persons (e.g. astronauts within a spacecraft) due to their exposure to a particular radiation field, the simple determination of the actual "absorbed dose" (i.e. the net energy deposited per unit mass) by itself as measured in an unknown mixed radiation field, does not necessarily provide the information needed to predict the risk of harm to a nearby individual. The reason is that given the vagaries of the energy loss mechanisms of the different components of an unknown charged particle radiation field, such a device can measure the same net absorbed dose for a wide variety of possible radiation environments that have widely varying potential risks associated with that particular exposure. Furthermore, the current state of the radiobiological understanding of exactly what risk can be associated with various long-term detrimental endpoints from different components of an incident radiation field is currently relatively limited (Cucinotta et al., 2015). As such, given the capabilities of a radiation-imaging device like the Timepix and its progeny, a more appropriate use is to focus on the detailed characterization of the radiation field. Then, as the radiobiology understanding of the effects continues to improve, such Timepix-like devices will continue to be relevant and lead to an increasing accuracy of the exposure risk assessment. Thus the continuing goal regarding the evolution of the detector technology is to provide information regarding the incident ambient radiation environment with a resolution that is sufficient to assess the risks using the then-current state of the radiobiology knowledge.

Having said that, the current Timepix-based devices can immediately provide accurate estimates of the various dosimetric quantities such as Absorbed Dose, and Dose-Equivalent as defined by NASA (Cucinotta et al., 2012), the NCRP (NCRP Report No. 153, 2006), (NCRP Report No. 142, 2002), (NCRP Report No. 137, 2001), (NCRP Report No. 132, 2000) and the ICRP (ICRP, 2013). Fig. 1 shows the Dose Equivalent Rate as a function of geographic location for a particular location in the ISS integrated over a period of several months recorded with USB-based "USB-Lite," from the Institute for Experimental and Applied Physics at the Czech Technical University in Prague (Vykydal and Jakubek, 2011), (referred to Radiation Environment Monitors or REM units by NASA). Calculation of the Dose-Equivalent typically requires knowledge of the Lineal Energy Transfer (LET) in tissue by each particle, something that can be measured by a Timepix-based device (e.g. in Silicon, and then corrected for the LET-dependent differences, especially at lower energies, between the LET in tissue and the LET in Silicon) (Linear energy transfer, 2018). Note that with such detailed characterization of the ambient radiation field, one can rely on transport codes (e.g. FLUKA (FLUKA), GEANT4 (Overview), PHITS (PHITS Home Page, 2018), or HZETRN (Hzetrn, 2015)) to propagate the incident radiation to predict the resulting environments within the astronaut's body, ultimately yielding a prediction of the Effective Dose. For example, in one current radiobiology approach the assessment of the risk contribution is based on the charge and energy (or velocity, β, as a fraction of the speed of light, c), on a particle-by-particle basis in each tissue type (Cucinotta et al., 2015; Whyntie and Harrison, 2015). Even Dose Equivalent formulations requiring such knowledge can be directly calculated from the data as measured by radiation imaging detectors. Note that the estimation of the LET is also one of the intermediate steps in estimating the charge and energy of each individual observed particle.

Having identified the knowledge of the charge and energy spectrum of the ambient charged particle flux, as the ultimately required values needed, the implementations of those capabilities will be discussed in more detail. However, these measurements are confined to the ambient charged particles. In space radiation environments there necessarily are neutrons and, to a lesser degree, high-energy photons. This is due to the fact that astronauts in space generally must be surrounded by other material such as spacecraft, habitats, or space suits, and subject to albedos coming from nearby objects such as the Moon, the Earth's atmosphere or any other significant nearby material. The detection of neutrons pose a somewhat different problem than high-energy photons, but the measurement of both by Timepix-based devices not be covered in this review article. (Neutron Detection) Of course, the ultimate assessment of the net risks from the total radiation exposure must include the contributions from all sources.

2. Timepix-based detectors

The design and function of the Timepix ASIC and the details of its' operation have been well documented elsewhere (Llopart et al., 2007) and in other articles within this Journal's edition. However, suffice it to say that in general the uses to date of the applications reviewed in this

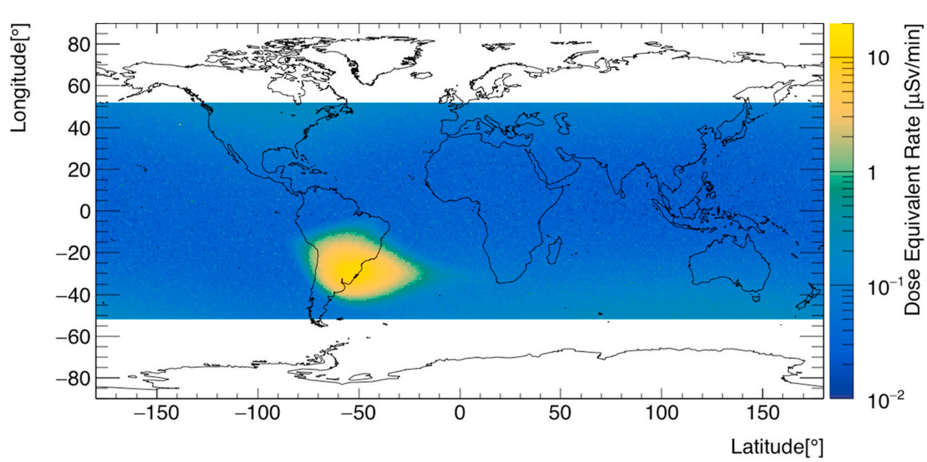

Fig. 1. The plot is a summary of the Dose-Equivalent (NCRP 142) rate averaged over November and December 2018 as measured by one of the Timepix-based devices onboard the ISS that were supplied to NASA by the Institute for Experimental and Applied Physics in Prague, Czech Republic.

paper generally employ 300–500 μm thick bulk n-type Silicon sensors with p-type implants isolating the connections to the solder pads, which are bump-bonded to the Timepix ASIC using the Flip-Chip® technology. The sensor top has a reverse-biased voltage with respect to the individual pixel solder pads that is sufficient to deplete the entire sensor volume of free charge carriers. The deposition of energy by charged particles moving through the sensor volume results in the excitation of electrons and their corresponding holes being elevated into the conduction band, and subsequently the holes will be attracted towards the Timepix pixel inputs by the bias voltage. The separation of free charges in the sensor volume induces a mirror image charge on the pixel inputs and the current induced in each pixel's charge-sensitive front-end pre-amplifier to supply that image charge is integrated to be digitized using the Time-Over-Threshold (TOT) (Knoll and Wilkinson, 1989) method. When the device is properly calibrated, the value of the digitized charge directly provides a measurement of that net portion of the energy deposited in the sensor that was collected in that pixel. Typically for most incident charged particles a cluster of multiple associated pixels share the collection of the induced charges creating a projection of the particle's track onto the pixel matrix. Most applicable space radiation environments are sparse enough to allow the detector to be read out in frames that are >1 s in duration, with a few rare situations that can require frame times as short as 10 ms. Operating algorithms have been deployed that dynamically adjust the frame duration with reference to several of the immediately previous frames to limit the nominal pixel occupancy to <4% (Stoffle et al., 2015).

3. Advanced energy calibration of the Timepix pixels

Measuring the LET for an energetic penetrating particle in a Timepix-based device with a Silicon sensor consists of two parts, estimating the length of the track in the sensor and the examining the details of the energy deposited along the projected track during the passage of that particle. Both steps have been the subjects of extensive efforts to optimize their resolution. In the case of slowing or stopping particles where the LET is changing noticeably along the projected track within the detector, a more detailed analytical procedure is required. However, all of these measurements ultimately rely on the accurate estimation at the level of the individual pixels of the net fraction of the energy loss by the particle that is represented by the TOT recorded value in each affected pixel.

For many applications a standard calibration procedure has been developed that does a 4 parameter fit to a relatively linear function with a near threshold "knee". This procedure employs sources and provides reasonable accuracy through charge collections that represent per pixel energy depositions up to ~1.1 MeV deposited in the sensor (Jakubek, 2011; Kroupa et al., 2012). However, the incident Galactic Cosmic Ray (GCR) flux includes occasional heavy ions with energies and charges that can contribute energy LETs in Si that reach 500 keV/μm. These extreme cases cause the front-end preamplifiers in the pixels to operate in unintended ways leading to oscillations and highly non-linear and multi-valued behavior.

Even with the highly non-linear behavior for larger pixel inputs, an "Advanced Calibration" procedure has been developed employing the use of the Van der Graff accelerator at the Brookhaven National Laboratory in New York (Kroupa et al., 2017b). This procedure involves exposing the detector to stopping proton beams in a beam-line vacuum target chamber, in order to deposit accurately known amounts of charge in the sensor. The analysis begins by examining the response of single pixel "clusters" where presumably only charges below the pixel thresholds are leaked to the surrounding pixels. This allows a careful scan of high charge pixel inputs. Once the response has been mapped initially from the single pixel clusters, it can be verified and adjusted by examining at the 2, 3 and 4 pixel charge-shared clusters.

At the highest charge depositions, the pixel output tends to plateau at a value below the calibrated peak (sometimes referred to a the "volcano effect," since these high values occur in the central regions of the cluster that are typically surrounded by "rim" pixels with higher values). An algorithm has been developed to estimate the amount of "missing charge from the number of "volcano" pixels and their extent and distribution using the data from the surrounding rim pixels.

4. Polar and azimuthal angle determination

One of the key parameters involved in the analysis procedure is the polar angle of the track with respect to the plane of the detector. "Vertical" tracks, those that are incident relatively perpendicular to the plane of the detector, are the most problematic (Hoang et al., 2014; Stoffle and Pinsky, 2018). While reasonable estimates for the track lengths and the total energy deposited can be determined, even with the loss of precision in determining the actual polar angle of the track, the issue is that because of the Bragg Peak in the LET, vertical stopping particles, especially for protons, can mimic more energetic and higher charged fully penetrating particles. The simplest solution to avoid such ambiguities is to limit the acceptance for analysis purposes to tracks with larger polar angles depending on the sensor thickness. In cases where heavier ion tracks are involved, the increasing ability to use the presence of longer-range delta rays to reveal that a higher-energy penetrating particle is present, may be able to regain some of the polar angle acceptance.

5. Particle charge and kinetic energy identification

For the tracks with polar angles ~60° and higher the track length, and thus the polar angle can be determined with considerable precision (Kroupa et al., 2018). In addition, once the azimuthal axis of the track has been identified, the track can be segmented into multiple section slices along the track to obtain a profile of the LET values along the track. Since slower particles below several hundred MeV will have an increasing LET as they slow down, maximum likelihood fits to the shape and size of the segmented profile can be used to estimate both the charge and energy of the incident particle. This procedure has attained a reasonable accuracy in assigning each track to a charge and energy bin (George et al., 2018).

Given the dominant relative abundances of Hydrogen and Helium in the incident fluxes, and their overlapping of LET values for relatively low total kinetic energies, it can be difficult to identify one from the other in the nominal single-layer Timepix Silicon sensors. While protons and helium nuclei have similar net LET values at the same velocity, the total kinetic energy of the Helium nuclei is 4-times that of the protons. This means that the protons will decelerate faster than the Helium, allowing one to discriminate between them by evaluating the change in LET over some pathlength. One efficient method of distinguishing them is to use 2 detectors with some amount of absorber material in between. To examine that, a Miniature Particle Telescope employing a stack consisting of two aligned Timepix detectors is currently being evaluated on the International Space Station (ISS).

6. Summary

Over the past decade, Timepix-based devices have been exceptionally successful being used in a wide variety of application in mixed radiation fields including their very successful adaptation to the challenges of the deployment in space to measure the ambient radiation environment both within spacecraft (see Fig. 1) and in free space. Ground-based mixed field applications are also continuing to evolve successfully as well. Even as we approach the dawn of the Timepix2 from the Medipix2 Collaboration, the venerable Timepix will continue to be a significant presence for years to come …

Declaration of competing interest

The authors declare that they have no known competing financial interests or personal relationships that could have appeared to influence the work reported in this paper.

Acknowledgments

This work was supported by KBR Human Health and Performance Contract (HHPC) NNJ15HK11B.

References

Caresana, M., Garlati, L., Murtas, F., Romano, S., Severino, C.T., Silari, M., 2014. Real-time measurements of radon activity with the Timepix-based RADONLITE and RADONPIX detectors. J. Inst. Met. 9, P11023.

Cucinotta, F.A., Kim, M.-H.Y., Chappell, L.J., 2012. Space Radiation Cancer Risk Projections and Uncertainties. NASA/TP-2013-217375.

Cucinotta, F.A., Alp, M., Rowedder, B., Kim, Myung-Hee Y., 2015. Safe days in space with acceptable uncertainty from space radiation exposure. Life Sci. Space Res. 5, 31–38.

The Official FLUKA Site: Fluka Home," http://www.fluka.org/fluka.php, (Viewed 18, October, 2018).

George, S.P., Kroupa, M., Wheeler, S., Kodaira, S., Kitamura, H., Tlustos, L., Campbell-Ricketts, T., Stoffle, N.N., Semones, E., Pinsky, L., 2018. Very high energy calibration of Silicon Timepix detectors. J. Inst. Met. 13, 11014.

Granja, C., Polansky, S., Vykydal, Z., Pospisil, S., Owens, A., Kozacek, Z., Mellab, K., Simcak, M., 2016. The SATRAM Timepix spacecraft payload in open space on board the Proba-V satellite for wide range radiation monitoring in LEO orbit. Planet. Space Sci. 125, 114–129.

Granja, C., Jakubek, J., Polansky, S., Zach, V., Krist, P., Chvatil, D., Stursa, J., Sommer, M., Ploc, O., Kodaira, S., Martisikova, M., 2018. Resolving power of pixel detector Timepix for wide-range electron, proton and ion detection. Nucl. Instrum. Methods A 908, 60–71.

Hoang, S.-M., August 2014. A Pattern Recognition Approach to Learning Tracks of Heavy-Ion Particles in Timepix Detectors. Ph.D. Computer Science, Dissertation. University of Houston, Houston, Texas, USA.

Hzetrn, 2015. Software Details. https://software.nasa.gov/software/LAR-18803-1 (Viewed 18 October 2018).

ICRP, 2013. Assessment of radiation exposure of astronauts in space. ICRP publication 123. Ann. ICRP 42 (4).

Jakubek, J., 2011. Precise energy calibration of pixel detector working in time-over-threshold mode. Nucl. Instrum. Methods A 633, S262.

Knoll, G.F., 1989. Radiation Detection and Measurement. In: Wilkinson, D.H. (Ed.), second ed. John Wiley & Sons, " New York, ISBN 0471815047, pp. 716–720. Proc. Cambridge Philoso. Soc. 46 Pt3 (1950) 508.

Kroupa, M., Jakubek, J., Soukup, P., 2012. Optimization of the spectroscopic response of the Timepix detector. J. Inst. Met. 7, C02058.

Kroupa, M., Bahadori, A., Campbell-Ricketts, T., Empl, A., Hoang, S.-M., Idarraga-Munoz, J., Rios, R., Semones, E., Stoffle, N., Tlustos, L., Turecek, D., Pinsky, L., 2015. A semiconductor radiation imaging pixel detector for space radiation dosimetry. Life Sci. Space Res. 6, 69–78.

Kroupa, M., Stoffle, N.N., Hoang, S., Idarraga-Munoz, J., Pinsky, L.S., 2017a. Modern semiconductor pixel detectors used as radiation Monitors. Solid-State Rad. Detect.: Technol. Appl. 1–16.

Kroupa, M., Campbell-Ricketts, T., Bahadori, A., Empl, A., 2017b. Techniques for precise energy calibration of particle pixel detectors. Rev. Sci. Instrum. 88 (3), 033301.

Kroupa, M., Zeitlin, C., Bahadori, A., Campbell-Ricketts, T., George, S.P., 2018. Kinetic energy reconstruction with a single layer particle telescope. Appl. Phys. Lett. 112, 134103.

Kubančák, J., Ambrožová, I., Pachnerová Brabcová, K., Jakůbek, J., Kyselová, D., Ploc, O., Bemš, J., Štěpán, V., Uchihori, Y., 2015. Comparison of cosmic rays radiation detectors on-board commercial jet aircraft. Radiat. Protect. Dosim. 164, 484–488.

Linear energy transfer – Wikipedia," https://en.wikipedia.org/wiki/Linear_energy_transfer, (Viewed 18 October 2018); See also: "NIST: Introduction of ESTAR, PSTAR, and ASTAR," https://physics.nist.gov/PhysRefData/Star/Text/intro.html. (Viewed 18 October 2018).

Llopart, X., Ballabriga, R., Campbell, M., Tlustos, L., Wong, W., 2007. Timepix, a 65k programmable pixel readout chip for arrival time, energy and/or photon counting measurements. Nucl. Instrum. Methods A 581, 485.

Ncrp Report No 132, 2000. Radiation Protection Guidance for Activities in Low-Earth Orbit. National Council on Radiation Protection and Measurements. ncrp@ncrponline.Org (Viewed 18 October 2018).

Ncrp Report No 137, 2001. Fluence-Based and Microdosimetric Event-Based Methods for Radiation Protection in Space.

Ncrp Report No 142, 2002. Operational Radiation Safety Program for Astronauts in Low-Earth Orbit: A Basic Framework. In: – ".

Ncrp Report No 153, 2006. Information Needed to Make Radiation Protection Recommendations for Space Missions beyond Low-Earth Orbit. ISBN-13: 978-0-929600-90-1.

Insert Reference to Neutron Detection(Article in this volume…)].

Overview | geant4.web.cern.Ch," https://geant4.web.cern.ch/, (Viewed 18 October 2018)..

PHITS Home Page," https://phits.jaea.go.jp/, (Viewed 18 October 2018)..

Pinsky, L., Idarraga-Munoz, J., Kroupa, M., Son, H.M., Stoffle, N.N., Semones, E.J., Bahadori, A.A., Turecek, D., Posposil, S., Jakubek, J., Vykydal, Z., Kitamura, H., Uchihori, Y., 3/2014. Medipix in space onboard the ISS. J. Radiat. Res. 55 (Suppl. 1), i62–i63.

Ploc, O., Kubancak, J., Sihver, L., Uchihori, Y., Jakubek, J., Ambrozova, I., Molokanov, A., Pinsky, L., 2014. Dosimetry measurements using Timepix in mixed radiation fields induced by heavy ions; comparison with standard dosimetry methods. J. Radiat. Res. 55, i141–i142.

Reference to Neutron and Photon Spectroscopy Article in the Same Volume].

See e.g. https://en.wikipedia.org/wiki/Cosmic_ray and references therein. (Viewed October 10, 2018).

Semones, Edward, April . Space Radiation Analysis Group. NASA/JSC, Houston, TX, USA. Personal Communication.

Stoffle, Nicholas, December 2013. Development of a Space Radiation Dosimeter Based on the Medipix2 Technology. Ph.D. Physics, Thesis. University of Houston, Houston, Texas, USA.

Stoffle, N., Pinsky, L., 2018. Identification of stopping ions in a Silicon Timepix detector. Nucl. Inst. and Meth. A880, 35–39.

Stoffle, N., Pinsky, L., Kroupa, M., Hoang, S., Idarraga, J., Amberboy, C., Rios, R., Hauss, J., Keller, J., Bahadori, A., Semones, E., Turecek, D., Jakubek, J., Vykydal, Z., Pospisil, S., 2015. Timepix-based radiation environment monitor measurements aboard the International Space Station. Nucl. Instrum. Methods Phys. Res. 782, 143–148.

See "Van Allen Radiation Belt," https://en.wikipedia.org/wiki/Van_Allen_radiation_belt, (viewed October 18, 2018).

Vykydal, Z., Jakubek, J., 2011. USB Lite—miniaturized readout interface for Medipix2 detector. Nucl. Instrum. Methods Phys. Res., Sect. A, Accel. Spectrom. Detect. Assoc. Equip. 633 (Suppl. 1), S48–S49.

Whyntie, T., Harrison, M.A., 2015. Full simulation of the LUCID experiment in the Low Earth Orbit radiation environment. J. Inst. Met. 10, C03043.

Further reading

Pinsky, L., Stoffle, N., Empl, A., Jakubek, J., Pospisil, S., Leroy, C., Kitamura, H., Yasuda, N., Uchihori, Y., 2011. Application of the Medipix2 technology to space radiation dosimetry and hadron therapy beam monitoring. Radiat. Meas. 46, 1610–1614.